Hindawi
Shock and Vibration
Volume 2023, Article ID 4645101, 11 pages
https://doi.org/10.1155/2023/4645101

Research Article

Experimental Study on Frequency Modulation Damping Effect of Digital Detonator in Road Clearance Blasting

Jing Gao[1], **Ping Cheng**[2], **Jian-Jun Ren**[3] **and Fengnian Wang**[4]

[1]*Yan'an Xing'an Blasting Engineering Service Co., Ltd, Yan'an, Shaanxi 716000, China*
[2]*School of Resource Engineering, Xi'an University of Architectural Science and Technology, Xi'an, Shaanxi 710055, China*
[3]*College of Physics and Engineering, Xingyi Normal University for Nationalities, Xingyi, Guizhou 562400, China*
[4]*Shanxi Transportation Technology Research & Development Co., Ltd., Taiyuan 30032, China*

Correspondence should be addressed to Ping Cheng; chengp_314@163.com

Received 23 February 2023; Revised 15 May 2023; Accepted 1 June 2023; Published 13 June 2023

Academic Editor: Iacopo Tamellin

To measure and evaluate the impact of vibration on the surrounding buildings and structures during highway rock burst removal and to formulate scientific and reasonable protective technical measures, the authors used the blasting perilous rock removal project of the K2227+920–K2228+000 section of the Shaanxi G316 road as a case study. The application of frequency modulation blasting vibration damping technology adopting digital electronic detonators was investigated. The difference in vibration peak and frequency between the perforation-by-hole initiation of the detonator and the frequency modulation initiation of the digital electronic detonator is compared. The results showed that by adopting an accurate delay of digital electronic detonators and the damping scheme of adjusting the blasting vibration frequency using the electronic detonators a reduction in blasting vibration velocity can be achieved. For an unchanged blasting scale, hole mesh parameters, and explosive unit consumption, the total blasting time was adjusted in the test. Compared to the hole-by-hole initiation, the blasting vibration velocity at a pier of the G85 Baohan highway bridge located 52 m away was reduced from 0.367 cm/s to 0.229 cm/s, a decrease of 36.7%. The field test demonstrated that frequency modulation and vibration attenuation using digital detonators can reduce blasting vibrations and effectively reduce the influence of blasting construction on surrounding buildings and structures.

1. Introduction

In recent years, numerous blasting accidents occurred during road clearance activities that caused significant economic losses and received bad press. Blasting in complex environmental conditions has become a challenging problem restricting engineering construction [1, 2]. The main risks to surrounding environment involved in road clearing blasting operations include vibrations, flying rocks, and air shock waves [3–5].

At present, there is a lack of systematic research on the influence of blasting operations carried out during road construction activities under complex environmental conditions on the surrounding environment [6–8]. Therefore, this study aims at closing this gap in knowledge. Blasting risks can be controlled and preempted depending on the specific environmental conditions encountered during construction, ensuring the safety of road clearing operations and reducing the interference with the surrounding environment. Under the same blasting vibration intensities, the lower the main vibration frequency, the closer it is to the self-vibration frequency of the protective object, and the greater the possibility of causing damage to the building (structure) [9, 10]. Therefore, by reducing the maximum detonation dosage of a single sound and shortening the delay time, the main vibration frequency can be effectively increased, so as to improve the safety of blasting vibration. If the delay between two holes is d, then the vibration spectrum of millisecond blasting has an obvious peak at the frequency of $1/d$ interval; by changing the delay interval, the frequency component of the blasting vibration can be changed, thus avoiding the self-vibration frequency band of the construction structure.

The use of a digital detonator makes the group holes detonate continuously at a very small jet lag difference, which is equivalent to adding blasting with a high base frequency as a forced vibration source, which causes the main vibration frequency in the near zone of blasting to tend to the base frequency of the vibration source, greatly improves the main vibration frequency, and reduces the possibility of resonance of building (construct).

This study adopted the K2227+920–K2228+000 perilous rock blast clearing project in the G316 road section in Shaanxi province as a case study. A damping scheme of the electronic detonator adjusting the actual blasting vibration frequency (frequency modulated damping) was studied with the aim of reducing blasting vibration velocity [11–13]. Using field tests, it was demonstrated that digital detonators can reduce blasting vibrations and protect the safety of buildings and other structures adjacent to the blasting site. This research will serve as a practical reference for scientific investigations and quantitative engineering design of road blasting operations in similar complex environmental conditions.

2. Project Background

2.1. Mechanism of the Electronic Detonator Priming System. The height of the building (above ground) exerts some amplification effect on the vibration velocity of blasting particles (in the horizontal direction), but the main frequency of blasting seismic waves has a significant impact on this amplification effect. Under the same conditions of blasting vibration intensity, the lower the main frequency, the closer it is to the natural frequency of the protected structure, and the higher the amplification rate of the particle vibration velocity, the greater the likelihood of causing damage to buildings (structures) [4, 5]. Methods such as reducing the maximum amount of initiating explosive per shot and shortening the delay time can effectively increase the main vibration frequency, thereby improving the safety of blasting operations.

The dependence of frequency on distance generally exhibits a negative exponential change, and due to the high-frequency filtering effect of soil, there will be a rapid decrease for high frequencies. Due to the fact that the low-frequency blasting vibration waves are close to the natural frequency of rock media, there will be a gentle decrease in low frequencies in the far-field region. The fundamental frequency of buildings is 3–10 Hz, derived from a shear cantilever model with a constant cross-section, and, based on the measured results, the following empirical formula for the natural vibration period of buildings (structures) is recommended:

$$T = 0.0168\left(H_0 + 1.2\right), \tag{1}$$

where T is the basic period, s, and H_0 is the calculation height of buildings (structures), m.

After the building (structure) is damaged by blasting vibrations, the natural vibration period will significantly increase in step with the severity of damage. Statistical data analysis shows that the period of a building (structure) after cracking may increase by 20% to 60% compared to the original structure.

Digital detonator frequency modulation shock absorption refers to the change in the total duration, intrahole delay, and interhole delay of blasting, which can be arbitrarily and accurately adjusted by using digital detonators placed in multiple blasting holes together with considering the actual rock mass engineering conditions. The vibration frequency of blasting and the difference in resonance frequency compared to the surrounding rock mass and buildings can be increased, while the cumulative effect of the main vibration phases of each group of seismic waves generated by each blasting hole charge is disrupted, to achieve dynamic shock absorption.

If the delay between each two blasting holes is d, then the vibration spectrum of millisecond blasting has a significant peak at every $1/d$ frequency interval; by changing the delay interval, the frequency component of blasting vibration can be changed, thereby avoiding the natural vibration frequency band of buildings (structures). By using digital detonators, when a group of blasting holes are continuously detonated with a small time difference, it is equivalent to adding a higher fundamental frequency blasting as a forced vibration source, resulting in the main vibration frequency of the blasting near the area tending towards the fundamental frequency of the vibration source, greatly increasing the main vibration frequency, reducing the possibility of resonance of building (structure) protective structures, and reducing the harm of blasting vibration.

2.2. Principle of Frequency Modulation Shock Absorption. Frequency modulation shock absorption using digital electronic detonators refers to multiple hole initiation according to actual engineering rock mass conditions. By changing the total blasting time, the initiation delay within a hole, and the delays between multiple holes, the blasting vibration frequency can be enhanced, increasing the gap between it and the resonance frequencies of the surrounding rock mass, buildings, and other structures. The coherence between the main vibration phases of the group of seismic waves generated by each blasting hole charge is disturbed, and dynamic shock absorption is achieved.

Compared to a large number of studies on blasting vibration particle peak velocity, only limited results on blasting vibration frequency are available [14–17].

The main frequency of blasting vibrations changes as the shock waves are attenuated away from the blasting center. To optimize the digital electronic detonator frequency modulation, the average frequency is adopted as the basis of engineering design. The definition of average frequency is as follows [18, 19]:

$$f_c = \frac{\sum_{i=1}^{n}\left(A_i f_i\right)}{\sum_{i=1}^{n} A_i}, \tag{2}$$

where f_c is the average frequency and A_i is the vibration velocity amplitude corresponding to frequency f_i.

Experiments showed that the attenuation of the average frequency of blasting vibration is more regular than that of the main frequency. An inverse power function was used to fit the data, and the correlation coefficient was close to 1, showing a significant correlation [20–24].

2.3. Project Overview. On February 17, 2018, the upper slope on the left-hand side of the G316 road in Wulipu Village (K2227+920–K2228+000), Wuguanyi Town, Liuba County suddenly collapsed. The collapsed material spilled onto the entire road surface and a part of it rushed into the nearby river. At present, the upper part of the slope is isolated, and the bedrock is overhanging, which poses a serious hazard to traffic safety and a threat to the substructure of a bridge located in the river on the right side of the highway along the G85 Baohan expressway.

The outcrop layer of this section of slope is Mesozoic granite. The rock mass is gray-yellow with a coarse crystal structure, massive structure, and well-developed joints and fissures. The mineral composition includes feldspar, quartz, and mica. The rock is relatively hard, and its integrity is relatively uncompromising.

The slope strata dip is 300°, and the dip angle is 45°. There are two main groups of joints: 140°∠85°: 2 pieces/m and 265°∠80°: 1 piece/m. The joints and strata cut the rock into blocks, which opened to form fissures after unloading.

The intended perilous rock blast clearance area is shown in Figure 1. It is about 8 m higher than the G316 road surface at Wulipu Village, Wuguanyi Town, Liuba County (K2227+920–K2228+000). Along the north side of G316 is the Bao River. According to the field investigations, the north side of the blasting construction area is 52 m away from the G85 Baohan Expressway bridge. There are residential houses on the west side of the intended perilous rock blast clearance area at a distance of at least 50 m. Six blasting vibration measurement points, denoted #1–#6, were arranged. Measurement points #1–#4 were arranged on the G316 road surface and measurement points #5 and #6 at the foundations of the adjacent expressway bridge piers, as shown in Figure 1.

On March 9, 2018, the Shaanxi Provincial Transportation Planning and Design Institute surveyed the site. The survey determined that the width of the slope is about 80 m and its height is about 60 m. There is still a large volume of perilous rock on the slope, and the crack width exceeds 20 cm. The collapse caused the upper part of the hill to lose support so that it now forms an overhang. The combined volume of slope perilous rock and hilltop loose rock is about 1200 m^3. The length of the adjacent rock mass is about 70 m, the width is 20–40 m, the thickness is 2–8 m, and the volume is about 1.47×10^4 m^3. The slope rock mass develops along stratified structural planes and opens inside the layer, forming an inverted slope. It is affected by gravity, rainfall, and heavy vehicle traffic vibrations, and there is a risk of further collapse of rock strata and joints.

According to the construction drawings of G316 Road Section K2227+920–K2228+000 Major Water Damage Repair Project compiled by the Shaanxi Transportation Planning and Design Institute in April 2020, the right hand side overhanging rock (route K2227+955–K2227+985 left) along the fracture surface (rock joint fracture inclination 45°) was cleared by blasting. The clearing range was from the left side to the boundary of the collapsed slope, from the right side to the gully, from the lower side to the road surface about 8 m high, and from the top to the top of the hill or no inverted slope. The maximum clearance thickness was 9.5 m, and the total clearance volume was about 7000 m^3, as shown in Figure 2 for a photographic view.

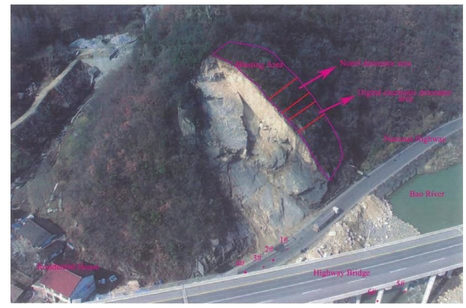

Figure 1: Blasting area surroundings.

3. Blasting Test Program

In the test, the blasting vibration monitoring data of the first and second blasting constructions in the blasting clearance area were selected for analysis. In the first experiment, the detonators initiated hole-by-hole, whereas in the second experiment, a digital electronic detonator frequency modulation vibration reduction plan was implemented, as shown in Figure 1.

3.1. Analysis of Blasting Conditions and Experimental Design. The main hazards related to blasting operations include blasting vibrations, flying rocks, harmful gases, blasting shock waves, noise, and dust [3]. Considering the surrounding environment of this blasting project, the main risk was deemed to be blasting vibrations.

3.1.1. Analysis of Possible Hazards Caused by Blasting Vibrations

① The main structure at risk of damage due to blasting vibrations in this project was the G85 Baohan Expressway bridge, which was 52 m away.

② After the explosive material is detonated, a generated stress wave will propagate through the rock or soil layer. When the local seismic wave intensity is greater than the strength of rock mass, it will cause damage and cracking [25–27]. Blasting damage may gradually accumulate[28], until the pier foundation of G85 Baohan Expressway bridge eventually becomes unstable.

③ Blasting vibrations can cause the opening, extension and transfixion of original cracks in the rock subgrade slope [15]. As a result, large rock fragments

Figure 2: Cleared perilous rocks.

may roll down the slope and impact the G85 Baohan Expressway bridge piers.

If the influence of the blasting vibrations exceed the safe thresholds, they will cause the foundation and walls of the nearby residential homes located 50 m away to crack and potentially fall [3, 29].

3.1.2. Design Principles. The blasting construction requirements are demanding and the surrounding conditions are complex. To ensure safe and efficient blasting, the digital electronic detonator hole-by-hole initiation system was implemented to achieve frequency modulation shock absorption, by precise control of explosive energy release, medium movement, crushing and damage accumulation [30], and reduce the amount of flying rocks [31].

3.2. Blasting Parameters Design. The adjacent rock mass is about 70 m long, 20–40 m wide, 2–8 m thick, and its dip angle is about 45°. According to the principles of hole layout, 70 mm diameter vertical holes in a triangular layout were adopted in the blasting area [32–35]; see Figure 3.

The charge holes were perpendicular to the surface of the rock mass, hole spacing was A (m) × row spacing B (m) = 1.0 m × 1.0 m, resistance line $W = 1.0$ m, west control resistance line was ≥1.2 m, and east resistance line was ≤1.0 m. Considering the perilous rock thickness of 2–8 m, the drilling was carried out to leave a 0.3 m thick protective layer from the bottom of the hole to the main joint slide surface [36]. The average unit explosive consumption was less than 0.55 kg/m^3. The blasting parameters designed for the hole depth of 6.0 mare shown in Table 1.

3.3. Blasting Sequence

3.3.1. Detonation Tubes Detonated Hole-by-Hole. Considering the rock mass properties, the delay time between holes was selected as 25 ms (MS2), the delay time between rows as 75 ms (MS4), and the delay time of charge in holes as 460 ms (MS11). Because the actual and the nominal delay of detonator have large discreteness [37–39], there is normally a delay error. Therefore, in the actual initiation process, a hole-by-hole initiation with a small delay time was adopted [40–43]. The time settings of hole initiation sequence are shown in Figure 4.

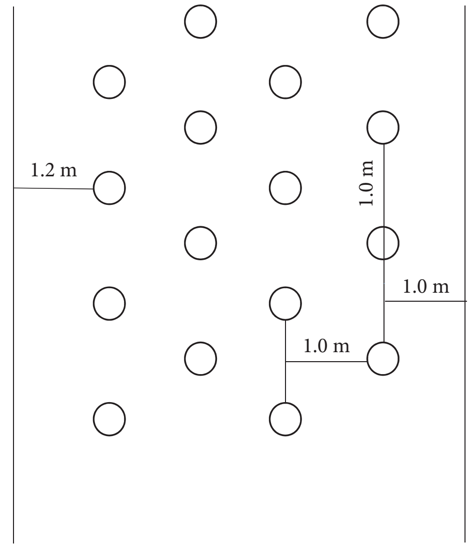

Figure 3: Schematic diagram of hole layout.

Table 1: Blasting hole array parameters.

Blasting parameters	Design values
Critical thickness (m)	2–8
Hole depth (m)	1.7–7.7
Aperture (mm)	70
Rock angle (°)	Perilous rock inclination 45
Hole dip angle (°)	Vertical perilous rock surface
Line of least resistance (m)	East side ≤ 1.0; west side ≥ 1.2
Pitch (m)	1.0
Array pitch (m)	1.0
Block length (m)	≥1.5
Unit explosive consumption (kg/m$^{3)}$	0.55
Single hole dosage (kg)	0.935–4.235

3.3.2. Digital Electronic Detonator Frequency Modulation Initiation. This scheme adopted hole-by-hole initiation combined with a millisecond delay within each hole. Considering the properties of rock mass, the delay between holes was assumed as 6 ms, the delay between rows as 27 ms, and the delay between charge packets in a hole as 5 ms. The setting of hole delay 6 ms and row delay 27 ms was determined according to the crushing effect of hole distance 1.0 m and row distance 1.0 m throwing effect test. The electronic detonator time settings of the uppermost charge pack in each hole are shown in Figure 4.

If the amount of charge in a hole exceeded 2.0 kg, an interval charge was adopted [21] by dividing the 2.0 kg charge pack into sections. The drug package was filled at a 1.0 m interval, and the delay from the orifice to the bottom of the hole was 5 ms.

4. On-Site Monitoring of Blasting Vibrations

4.1. Layout of Measurement Points. The EXP3850 blasting vibration instrument manufactured by Chengdu Zhongke Dynamic Instrument Co., Ltd. was adopted in this study together with velocity sensors, which collected, stored, and analyzed data from the tangential, vertical, and radial

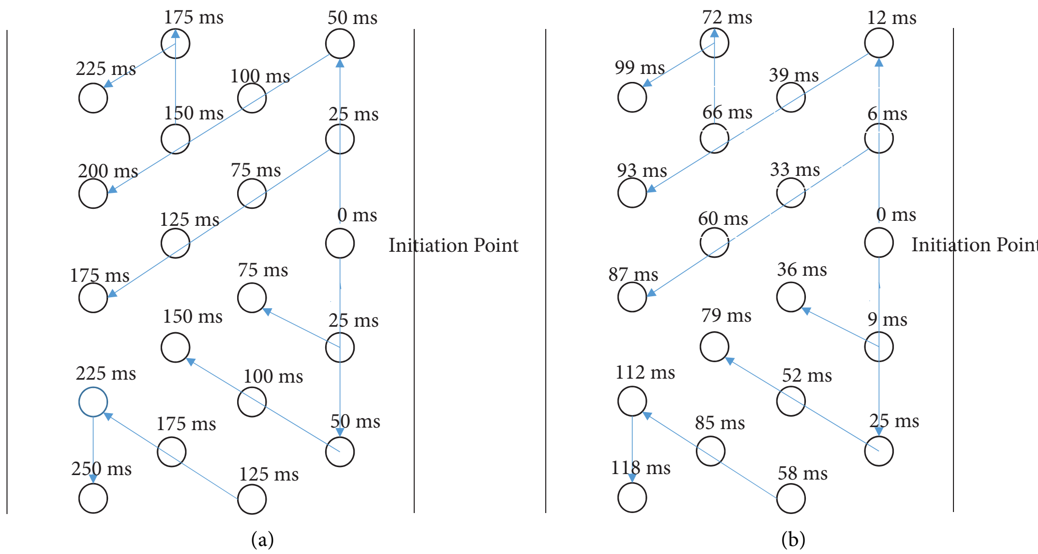

Figure 4: Schematic diagram of the detonation array. (a) Hole-by-hole initiation of the detonating tube (surface initiation time: 250 ms). (b) Digital electronic detonator initiation (surface initiation time 118 ms).

channels. The EXP3850 blasting vibration recorder is a portable instrument that can record and analyze the seismic waveform signals caused by blasting [44]. The instrument was directly connected to the velocity sensors and placed near each measurement point. The instrument can automatically record eight vibration events and their occurrence times and pass data through an RS232 interface to a computer for data processing.

The arrangement of measurement points plays a very important role in blasting vibration testing, because it directly affects the observed data [45, 46]. The number and location of measurement points are determined mainly according to the purpose of testing and field conditions. The arrangement of measurement points should follow the following principles [47]:

(1) To determine the impact of blasting vibrations on the expressway bridge piers and residential house foundation, representative measurement locations should be selected.

(2) The selected test site has uniform geological conditions and essentially the same lithology. Near a large fault zone, the measurement points should be arranged on one side of the fault or fracture zone.

(3) The observed data can reflect the variation in seismic wave characteristics.

The measurement points in this experiment were arranged on the highway bridge piers and highway foundation, as shown in Figure 5. The relative positions of measurement points are shown in Table 2.

4.2. Vibration Data Analysis. The vibration velocity of a rock-soil medium can be decomposed into three mutually perpendicular directions:vertical, horizontal radial, and horizontal tangential [3]. A vector synthesis waveform in three directions was shown as Figure 6.

The spectrum and power spectrum wave forms in the X, Y, and Z directions of measuring point 3 with moderate location and blasting vibration velocity were selected for analysis and explanation. The monitoring data are shown in Figure 7.

From the spectrum and power spectrum in the three directions of X, Y, Z of measurement point 3, it can be seen that the energy is mainly concentrated in the frequency band of 20~30 Hz and 30~60 Hz only has less energy. Moreover, the power spectrum shows that the energy of the blasting seismic wave is concentrated in the lower frequency band and is mainly concentrated in the 20~25 Hz frequency band, as shown in Figure 7. And also from the power spectrum in the Z direction, it can be seen that the energy of the signal develops towards high frequencies and energy distribution widens. In addition, there are many subfrequency bands in the range of 25~100 Hz, and the energy peaks of each subband are not much different.

It can be seen from the original power spectrum that the energy frequency of the blasting vibration signal is mainly a low-frequency signal below 30 Hz, and a small part of the other part is 40~100 Hz. The main reason is related to the blasting vibration signal propagation medium in the construction area, and the high-frequency signal is easy to filter out or attenuate in the formation, and on the other hand, the wave guide effect and the layered formation can propagate the Z-direction frequency farther.

The half-wave frequency corresponding to the peak of blasting vibration is called the apparent dominant frequency, which can better reflect the frequency characteristics of blasting vibrations [19]. As shown in Figure 8, the apparent dominant frequency of blasting vibration at each measurement point increased with the horizontal distance from the blasting center, and the variations in the apparent dominant frequency in the three directions show a general attenuation trend. Table 3 shows the vibration

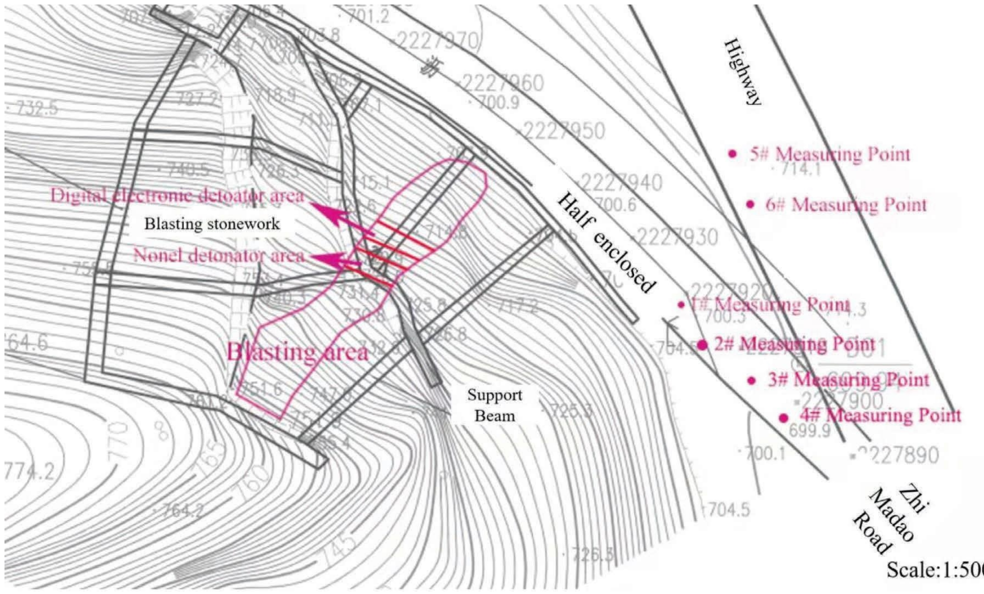

Figure 5: Measurement point layout.

Table 2: Relative position of blasting vibration measurement points.

Measurement points	Distance from detonation center (m)	
	Horizontal distance	Vertical distance
#1	41.5	24.1
#2	52.3	24.0
#3	70.3	23.4
#4	84.5	23.8
#5	56.2	27.5
#6	67.2	27.6

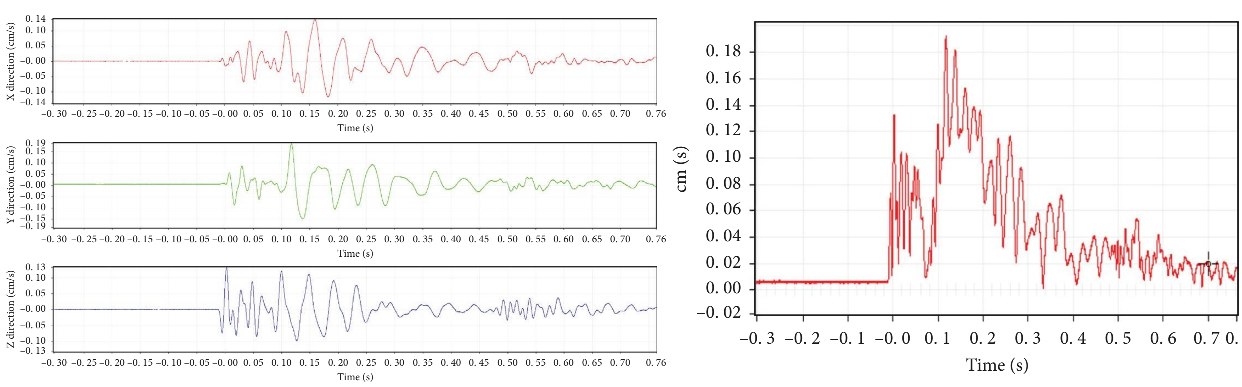

Figure 6: Horizontal radial (X) tangential (Y) vertical (Z) vector synthesis waveform diagram.

monitoring statistics with adjusted total blasting time, intrahole delay, and interhole delay by adopting the digital electronic detonator initiation system. The main vibration frequency was between 30 Hz and 60 Hz. The average frequency in the three directions when the digital electronic detonator initiation system was used was 42.62 Hz, which was nearly 41% higher than the average frequency of 30.28 Hz in the three directions of the hole-by-hole initiation system [48].

According to the above monitoring data of blasting vibration velocity and field investigation, the Shaanxi G316 Liuba section K2227+920–K2228+000 perilous rock blasting removal project near the G85 Baohan Expressway bridge pier area did not have adverse effects on surrounding buildings and structures. The experimental results show that using the digital electronic detonator frequency modulated initiation system can reduce the blasting vibration velocity and ensure safe construction. [49].

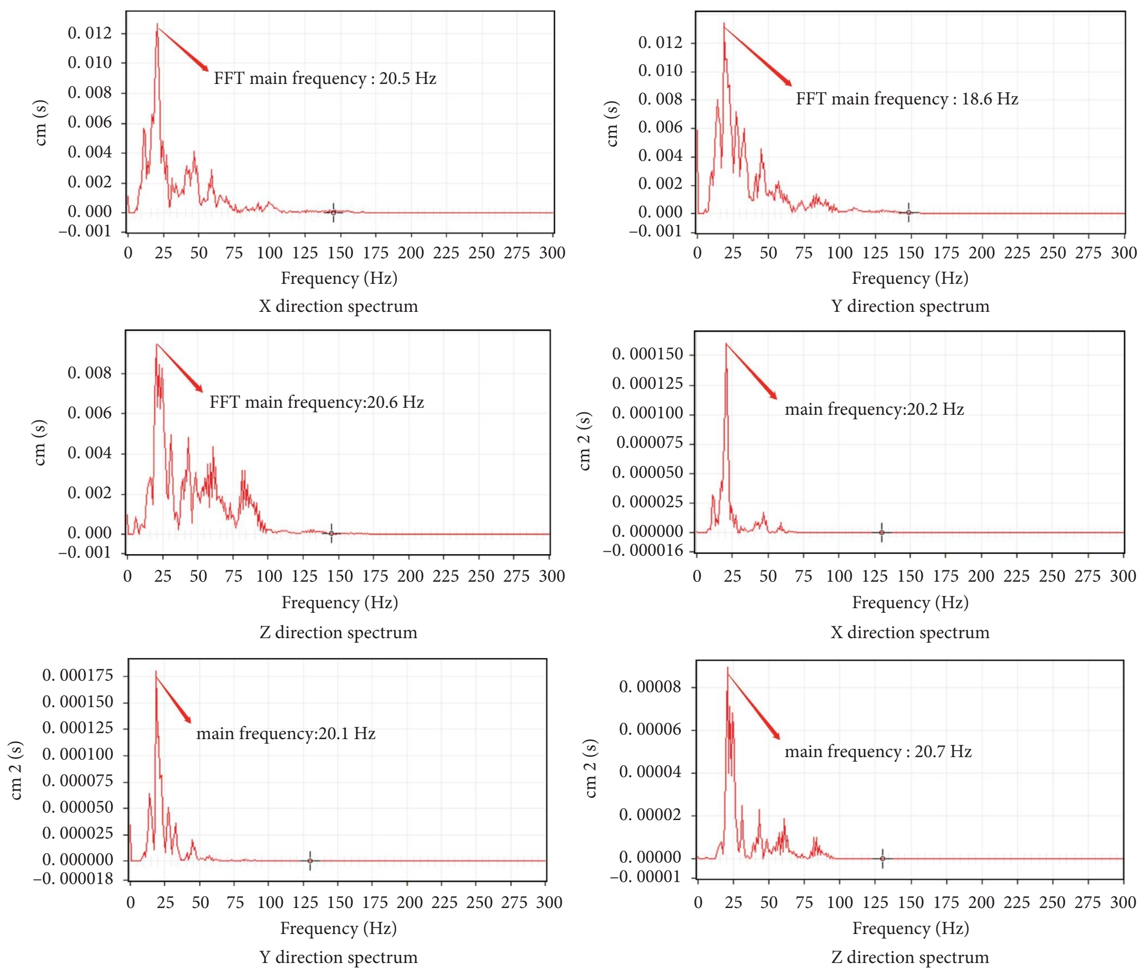

Figure 7: Analysis of blasting vibration velocity, frequency spectrum, and power spectrum of digital electronic detonator initiation about measuring point 3.

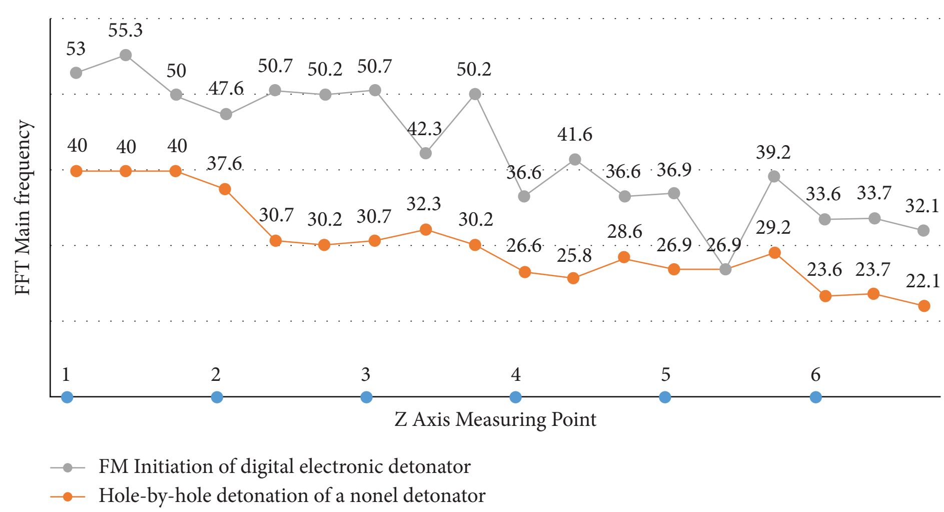

Figure 8: Comparison of dominant vibration frequencies between hole-by-hole initiation and frequency-modulated initiation using digital electronic detonators. Note: dominant frequency shown is for the Z-direction.

Table 3: Statistics of vibration monitoring data for digital electronic detonator initiation system.

Measurement points	Direction	Peak vibration velocity (cm/s)	FFT frequency (Hz)	Maximum time (s)	Strike (cm/s)	Sensor number
#1	X	0.3772	53.0	0.0433	0.017	EMI53924 151325.BST
	Y	0.2673	55.3	0.4446	0.017	
	Z	0.3051	50.0	0.2858	0.017	
#2	X	0.3145	47.6	0.0865	0.017	EMI53925 082031.BST
	Y	0.3132	50.7	0.0845	0.017	
	Z	0.3876	50.2	0.0877	0.017	
#3	X	0.1723	50.7	0.0454	0.017	EMI53928 151325.BST
	Y	0.2016	42.3	0.0332	0.017	
	Z	0.3432	50.2	0.1897	0.017	
#4	X	0.1656	36.6	0.2954	0.017	EMI53927 151137.BST
	Y	0.0754	41.6	0.3077	0.017	
	Z	0.1331	36.6	0.2643	0.017	
#5	X	0.1107	36.9	0.3336	0.017	EMI53926 175006.BST
	Y	0.1973	26.9	0.2847	0.017	
	Z	0.1813	39.2	0.2899	0.017	
#6	X	0.1166	33.6	0.4670	0.017	EMI53923 112505.BST
	Y	0.1262	33.7	0.3445	0.017	
	Z	0.2294	32.1	0.4753	0.017	

Table 4: Statistics of vibration monitoring data of the detonator and detonator.

Measurement points	Direction	Peak vibration velocity (cm/s)	FFT frequency (Hz)	Maximum time (s)	Strike (cm/s)	Sensor number
#1	X	0.4772	40.0	0.0453	0.017	EMI53924 151325.BST
	Y	0.3683	40.0	0.4496	0.017	
	Z	0.3052	40.0	0.2898	0.017	
#2	X	0.4182	37.6	0.3006	0.017	EMI53925 082031.BST
	Y	0.3083	30.7	0.2862	0.017	
	Z	0.4915	30.2	0.2899	0.017	
#3	X	0.2743	30.7	0.2952	0.017	EMI53928 151325.BST
	Y	0.2186	32.3	0.3030	0.017	
	Z	0.4489	30.2	0.2133	0.017	
#4	X	0.2618	26.6	0.0896	0.017	EMI53927 151137.BST
	Y	0.1756	25.8	0.0867	0.017	
	Z	0.3330	28.6	0.0898	0.017	
#5	X	0.2107	26.9	0.0452	0.017	EMI53926 175006.BST
	Y	0.1973	26.9	0.0346	0.017	
	Z	0.2893	29.2	0.0127	0.017	
#6	X	0.2166	23.6	0.4630	0.017	EMI53923 112505.BST
	Y	0.2262	23.7	0.0011	0.017	
	Z	0.3666	22.1	0.4582	0.017	

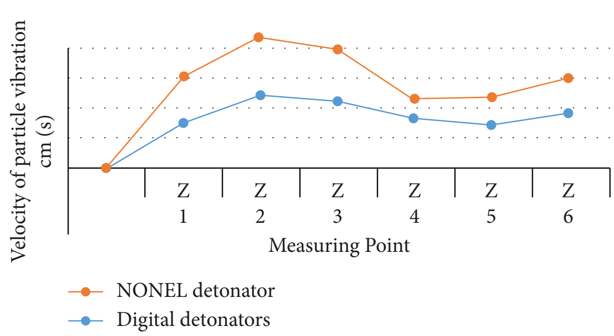

Figure 9: Comparison of peak vibration velocities between hole-by-hole initiation and frequency-modulated initiation using digital electronic detonators. Note: particle vibration velocity shown is the maximum velocity in Z.

The on-site blasting vibration monitoring results (see Tables 3 and 4) show that the blasting particle vibration peak velocities at all measurement points in all three directions were always less than the allowable threshold of 1.50 cm/s stipulated in blasting safety regulations GB6722-2014.

As shown in Figures 8 and 9, the dominant vibration frequency was between 20 Hz and 60 Hz [50, 51]. At measurement point #6 (placed at bridge pier foundations), the maximum frequency-modulated vibration velocity when the digital electronic detonator initiation system was used was 0.2294 cm/s. On the other hand, the maximum vibration velocity when the hole-by-hole detonation scheme was adopted was 0.3666 cm/s, thus, a reduction of 36.7% was achieved.

5. Conclusions

This paper used the Shaanxi G316 Road section K2227+920–K2228+000 perilous rock blast clearance project to investigate the application of digital electronic detonator frequency modulation shock absorption blasting technology. The in-situ test results showed that by using a precise digital electronic detonator delay scheme to adjust the actual vibration frequency of blasting vibrations (frequency modulated damping), it is possible to achieve a reduction in blasting vibration particle velocity. For unchanged blasting scale, hole array parameters and explosive unit consumption, by adjusting the total blasting time, digital detonator frequency modulated shock absorption can reduce blasting vibrations and guarantee better safety of surrounding buildings and structures compared to the traditional hole-by-hole initiation scheme.

The conclusions and recommendations of this research are as follows:

(1) Based on the resonant frequency of buildings and structures, the response frequency of blasting vibration, and the attenuation law of low-frequency blast wave propagation, the delay time between blastholes is adjusted using digital detonators to change the blasting vibration frequency, so as to achieve vibration reduction, which provides a basis for safe planning of road blasting construction projects under complex environmental conditions.

(2) By utilizing the high-precision and arbitrarily delayed time characteristics of digital detonators, a 5 ms in-hole delay is used to form a 3D in-hole charge initiation sequence through the joint action of the surface initiation network and in-hole initiation network during the initiation process of blasting. Experimental results have shown that good crushing and shock absorption effects can be achieved.

(3) According to the in situ monitoring data, the blasting interval between holes was reduced from 50 ms to 9 ms, the initiation time of the whole explosion area was reduced from 250 ms to 118 ms, the vibration frequency increased from 20 Hz to 40 Hz, and the intensity of the explosion source was reduced from 4.2 kg to 2.2 kg. At the pier of the G85 Baohan Expressway bridge located 52 m north from the blasting area, the blasting vibration velocity decreased from 0.367 cm/s to 0.229 cm/s, i.e., by 36.7%.

(4) The difference in timing accuracy between the digital detonator initiation system and the detonating network of the nonel detonator during the initiation process results in a change in the superposition of the residual stress of the first detonating charge and the explosive stress of the second detonating charge. The respective rock-breaking mechanisms are also different. If the blasting conditions are fixed, the digital detonator initiation system and the detonating network use the same initiation sequence. Due to the large timing error, the detonating network of the detonating tube disrupts the stress field, and the seismic effect of blasting is smaller than that of blasting using the digital detonator initiation system. Therefore, in the design and execution of blasting, the design rules of the detonator initiation network cannot be simply applied to the digital detonator initiation system.

Data Availability

The data used to support the findings of the study are available within the article.

Conflicts of Interest

The authors declare that they have no conflicts of interest.

Acknowledgments

This work was financially supported by the Youth Science and Technology Talent Growth Project of Guizhou Provincial Department of Education (Grant no. ky[2018]414). The authors would also like to thank EditSprings (https://www.editsprings.cn/) for the expert linguistic services provided.

References

[1] L. C. Zhu, "Cut excavation blasting in complex environmental conditions," *Engineering blasting*, vol. 8, no. 2, pp. 45–47, 2002.

[2] H. Tang, "Study on Safety technology of railway cutting blasting excavation under complex environment," *Engineering blasting*, vol. 25, no. 1, pp. 24–31, 2019.

[3] State Administration of Work Safety, *Safety Regulations for Blasting:GB 6722-2014*, China Standards Press, Beijing, China, 2015.

[4] N. Jiang, B. Zhu, X. He, C. Zhou, X. Luo, and T. Wu, "Safety assessment of buried pressurized gas pipelines subject to blasting vibrations induced by metro foundation pit excavation," *Tunnelling and Underground Space Technology*, vol. 102, Article ID 103448, 2020.

[5] M. Xu, X. Li, T. Liu et al., "A study on hollow effect and safety design of deep crossing caverns under blasting vibration," *Tunnelling and Underground Space Technology*, vol. 111, Article ID 103866, 2021.

[6] N. Dinh Dat, T. Quoc Quan, and N. Dinh Duc, "Vibration analysis of auxetic laminated plate with magneto-electro-elastic face sheets subjected to blast loading," *Composite Structures*, vol. 280, Article ID 114925, 2022.
[7] Y. Xia, N. Jiang, C. Zhou, and X. Luo, "Safety assessment of upper water pipeline under the blasting vibration induced by Subway tunnel excavation," *Engineering Failure Analysis*, vol. 104, pp. 626–642, 2019.
[8] B. Zhu, N. Jiang, C. Zhou, X. Luo, Y. Yao, and T. Wu, "Dynamic failure behavior of buried cast iron gas pipeline with local external corrosion subjected to blasting vibration," *Journal of Natural Gas Science and Engineering*, vol. 88, Article ID 103803, 2021.
[9] Y. Xia, N. Jiang, C. Zhou, X. Meng, X. Luo, and T. Wu, "Theoretical solution of the vibration response of the buried flexible HDPE pipe under impact load induced by rock blasting," *Soil Dynamics and Earthquake Engineering*, vol. 146, Article ID 106743, 2021.
[10] Y. Xia, N. Jiang, C. Zhou, J. Sun, X. Luo, and T. Wu, "Dynamic behaviors of buried reinforced concrete pipelines with gasketed bell-and-spigot joints subjected to tunnel blasting vibration," *Tunnelling and Underground Space Technology*, vol. 118, Article ID 104172, 2021.
[11] E. Dong, L. An, Y. Li, and C. Wu, "Hilbert spectrum analysis method of blast vibration signal based on HHT instantaneous phase optimization," *Applied Acoustics*, vol. 192, Article ID 108732, 2022.
[12] X. Huo, X. Shi, X. Qiu et al., "A study on raise blasting and blast-induced vibrations in highly stressed rock masses," *Tunnelling and Underground Space Technology*, vol. 123, Article ID 104407, 2022.
[13] X. Wang, J. Li, X. Zhao, and Y. Liang, "Propagation characteristics and prediction of blast-induced vibration on closely spaced rock tunnels," *Tunnelling and Underground Space Technology*, vol. 123, Article ID 104416, 2022.
[14] B. I. Weiguo and S. H. I. Chong, "Optimization selection of blasting vibration velocity attenuation formulas," *Rock and Soil Mechanics*, vol. 25, no. 1, pp. 99–102, 2004.
[15] H. Tang, Y. Shi, H. Li, J. Li, X. W. Wang, and P. C. Jiang, "Prediction of peak velocity of blasting vibration based on neural network," *Chinese Journal of Rock Mechanics and Engineering*, vol. 26, no. 1, pp. 3533–3539, 2007.
[16] N. Jiang, C. B. Zhou, W. Ping, X. Xu, and S. W. Lu, "Altitude effect of blasting vibration velocity in rock slopes," *Journal of Central South University*, vol. 45, no. 1, pp. 237–243, 2014.
[17] K. Iwano, K. Hashiba, J. Nagae, and K. Fukui, "Reduction of tunnel blasting induced ground vibrations using advanced electronic detonators," *Tunnelling and Underground Space Technology*, vol. 105, Article ID 103556, 2020.
[18] L. F. Trivino, B. Mohanty, and B. Milkereit, "Seismic waveforms from explosive sources located in boreholes and initiated in different directions," *Journal of Applied Geophysics*, vol. 87, no. 1, pp. 81–93, 2012.
[19] P. C. Sun, W. Lu, Z. Lei, M. Chen, R. Z. Li, and F. Q. Li, "Blasting vibration response and control of high rock slopes of thin mountain," *Chinese Journal of Geotechnical Engineering*, vol. 43, no. 05, pp. 877–885, 2021.
[20] D. Liu, W. B. Lu, M. Chen, and P. Yan, "Attenuation formula of the dominant frequency of blasting vibration during tunnel excavation," *Chinese Journal of Rock Mechanics and Engineering*, vol. 37, no. 9, pp. 2015–2026, 2018.
[21] J. Y. Li, Q. Kang, and M. S. Zhao, "Model tests on propagation laws of blasting vibration in jointed rockmass," *Blasting*, vol. 39, no. 2, pp. 30–35, 2022.
[22] R. Rodríguez, L. García de Marina, M. Bascompta, and C. Lombardía, "Determination of the ground vibration attenuation law from a single blast: a particular case of trench blasting," *Journal of Rock Mechanics and Geotechnical Engineering*, vol. 13, no. 5, pp. 1182–1192, 2021.
[23] X. Tian, Z. Song, and J. Wang, "Study on the propagation law of tunnel blasting vibration in stratum and blasting vibration reduction technology," *Soil Dynamics and Earthquake Engineering*, vol. 126, Article ID 105813, 2019.
[24] Y. Gou, X. Shi, J. Zhou, X. Qiu, X. Chen, and X. Huo, "Attenuation assessment of blast-induced vibrations derived from an underground mine," *International Journal of Rock Mechanics and Mining Sciences*, vol. 127, Article ID 104220, 2020.
[25] Z. Y. Zhang, N. H. Yang, W. B. Lu, G. Zhao, and F. Shi, "Progress of Blasting Vibration Control Technology in china," *Blasting*, vol. 30, no. 2, pp. 25–32, 2013.
[26] N. Jiang, Y. Jia, Y. Yao, J. Sun, B. Zhu, and T. Wu, "Experimental investigation on the influence of tunnel crossing blast vibration on upper gas pipeline," *Engineering Failure Analysis*, vol. 127, Article ID 105490, 2021.
[27] N. Jiang, B. Zhu, C. Zhou et al., "Blasting vibration effect on the buried pipeline: a brief overview," *Engineering Failure Analysis*, vol. 129, Article ID 105709, 2021.
[28] J. Silva, T. Worsey, and B. Lusk, "Practical assessment of rock damage due to blasting," *International Journal of Mining Science and Technology*, vol. 29, no. 3, pp. 379–385, 2019.
[29] W. Chun-lin and Z. Yi-ping, "Study on blasting vibration and its control technology," *Nonferrous Metals Design*, vol. 2, p. 36, 2009.
[30] R. Q. Eades and K. Perry, "Understanding the connection between blasting and highwall stability," *International Journal of Mining Science and Technoloy*, vol. 29, no. 1, pp. 99–103, 2019.
[31] R. Xie, X. Ren, L. Liu, Y. Xue, D. Fu, and R. Zhang, "Research on design and firing performance of Si-based detonator," *Defence Technology*, vol. 10, no. 1, pp. 34–39, 2014.
[32] D. P. Blair, "Approximate models of blast vibration in non-isotropic rock masses," *International Journal of Rock Mechanics and Mining Sciences*, vol. 128, Article ID 104245, 2020.
[33] J. Zhou, Y. Qiu, M. Khandelwal, S. Zhu, and X. Zhang, "Developing a hybrid model of Jaya algorithm-based extreme gradient boosting machine to estimate blast-induced ground vibrations," *International Journal of Rock Mechanics and Mining Sciences*, vol. 145, Article ID 104856, 2021.
[34] C. Cai, Q. Qian, and Y. Fu, "Application of BAS-Elman neural network in prediction of blasting vibration velocity," *Procedia Computer Science*, vol. 166, pp. 491–495, 2020.
[35] C. Fan and J. Ge, "Dynamic calculation method of vibration response of building blasting based on differential equation," *Environmental Technology & Innovation*, vol. 20, Article ID 101178, 2020.
[36] X. Wu, M. Gong, H. Wu, G. Hu, and S. Wang, "Vibration reduction technology and the mechanisms of surrounding rock damage from blasting in neighborhood tunnels with small clearance," *International Journal of Mining Science and Technology*, vol. 33, no. 5, pp. 625–637, 2023.
[37] G. Q. Zhang, "Hole-by-hole initiation network with nonel detonator," *Engineering blasting*, vol. 22, no. 3, pp. 27–30, 2016.
[38] Y. Gou, X. Shi, X. Qiu, X. Huo, and Z. Yu, "Assessment of induced vibrations derived from the wave superposition in time-delay blasts," *International Journal of Rock Mechanics and Mining Sciences*, vol. 144, Article ID 104814, 2021.

[39] D. Ren, J. Hou, J. Duan, Y. Ye, X. Liu, and D. Liu, “Failure Mode Analysis of Electronic Detonator under High Overload condition,” *FirePhysChem*, vol. 2, no. 2, pp. 199–205, 2022.

[40] S. Zhifei, K. Man, and L. Xiaoli, “Identifying delay time of detonator for a millisecond blasting,” *Advances in Civil Engineering*, vol. 2021, Article ID 5592696, 8 pages, 2021.

[41] P. [Wang, Y. Ma, Y. Zhu, and J. Zhu, “Experimental study of blast-induced vibration characteristics based on the delay-time errors of detonator,” *Advances in Civil Engineering*, vol. 2020, Article ID 8877409, 9 pages, 2020.

[42] F. Lin, R. Liu, Z. Zhang, D. Jiang, J. Chen, and Y. Li, “Reduction of blasting induced ground vibrations using high-precision digital electronic detonators,” *Frontiers in Earth Science*, vol. 9, 2021.

[43] X. Guan, C. Guo, B. Mou, and L. Shi, “Tunnel millisecond-delay controlled blasting based on the delay time calculation method and digital electronic detonators to reduce structure vibration effects,” *PLoS One*, vol. 14, no. 3, Article ID e0212745, 2019.

[44] Z. Wang, W. Gu, T. Liang, S. Zhao, P. Chan, and L. Yu, “Monitoring and Prediction of the Vibration Intensity of Seismic Waves Induced in Underwater Rock by Underwater Drilling and Blasting,” *Defence Technology*, vol. 18, no. 1, pp. 109–118, 2020.

[45] C. Huang, Z. Lei, and S. Y. Wei, “Evaluation and prediction of elevation blasting vibration based on AHP and normal distribution,” *Engineering Blasting*, vol. 8, no. 1, 2021.

[46] Y. Li and P. Jiang, “Prediction methods for blasting-induced ground vibration velocity,” *Journal of Vibration and Shock*, vol. 29, no. 5, pp. 179–182, 2010.

[47] D. Garai, H. Agrawal, and A. K. Mishra, “Study on impact of orientation of blast initiation on ground vibrations,” *Journal of Rock Mechanics and Geotechnical Engineering*, vol. 15, no. 1, pp. 255–261, 2022.

[48] P. Sun, W. Lu, J. Zhou, X. Huang, M. Chen, and Q. Li, “Comparison of dominant frequency attenuation of blasting vibration for different charge structures,” *Journal of Rock Mechanics and Geotechnical Engineering*, vol. 14, no. 2, pp. 448–459, 2022.

[49] X. Guan, L. Zhang, Y. Wang, H. Fu, and J. An, “Velocity and stress response and damage mechanism of three types pipelines subjected to highway tunnel blasting vibration,” *Engineering Failure Analysis*, vol. 118, Article ID 104840, 2020.

[50] H. Chu, X. Yang, S. Li, and W. Liang, “Experimental study on the blasting-vibration safety standard for young concrete based on the damage accumulation effect,” *Construction and Building Materials*, vol. 217, pp. 20–27, 2019.

[51] K. Wang, X. Qian, and Z. Liu, “Experimental and numerical investigations on predictor equations for determining parameters of blasting-vibration on underground gas pipe networks,” *Process Safety and Environmental Protection*, vol. 133, pp. 315–331, 2020.